

## TWO PHASE HEAT TRANSFER IN HORIZONTAL TUBE WITH JET MIXING

D. MUKHERJEE, M. P. SINHA\*, N. K. PUROHIT and A. K. MITRA

Department of Chemical Engineering, Indian Institute of Technology,  
Kharagpur-721302, India

(Received 24 August 1979 and in revised form 24 November 1979)

**Abstract** — The paper deals with experimental studies on heat transfer coefficients in two phase cocurrent flow in a horizontal tube where liquid jet momentum has been used for gas-liquid dispersion and heat transfer. Empirical equations have been developed to predict augmentation ratio of heat transfer as a function of various physical and dynamic variables of the system.

### NOMENCLATURE

$A_R$ ,	area ratio, $(D/d)^2$ ;
$c_p$ ,	specific heat of motive fluid;
$c'_p$ ,	specific heat of the secondary fluid;
$D$ ,	diameter of the tube;
$d$ ,	diameter of the nozzle;
$de$ ,	effective entry diameter, $(D - d)$ ;
$Eu$ ,	Euler number of the secondary fluid $\Delta P g_c / \rho' u'^2$ ;
$g_c$ ,	gravitational constant;
$h_{TP}$ ,	two phase heat transfer coefficient with jet mixing;
$h_F$ ,	single phase heat transfer coefficient of liquid without jet mixing;
$H$ ,	humidity of air;
$k$ ,	thermal conductivity of the motive fluid;
$k'$ ,	thermal conductivity of the secondary fluid;
$M$ ,	motive fluid mass flow rate;
$M'$ ,	secondary fluid mass flow rate;
$P$ ,	static pressure as denoted by subscripts;
$\Delta P$ ,	pressure difference, $P_0 - P_i$ ;
$Pr$ ,	Prandtl number of the motive fluid;
$Re_N$ ,	Reynold's number of motive fluid based on nozzle diameter;
$Re_T$ ,	Reynold's number of the motive fluid based on tube diameter;
$T$ ,	bulk temperature of fluid as denoted by subscripts;
$T'$ ,	temperature of the secondary fluid, as denoted by subscripts;
$u$ ,	jet velocity based on nozzle diameter;
$u'$ ,	velocity of the secondary fluid based on the effective entry diameter, $de$ ;
$V$ ,	volumetric flow rate of the motive fluid;
$V'$ ,	volumetric flow rate of the secondary fluid;
$x$ ,	axial distance along the length of the test section from the point of entry to the section;
$\rho$ ,	density of the motive fluid;
$\rho'$ ,	density of the secondary fluid;

$\mu$ ,	viscosity of the motive fluid;
$\mu'$ ,	viscosity of the secondary fluid.

### Subscripts

$av$ ,	average;
$s$ ,	sections 1, 2, 3, 4 and 5;
$i$ ,	inlet to the test section;
$o$ ,	outlet to the test section;
$w$ ,	wall.

### INTRODUCTION

THE USE of jet mixing phenomena for creating high turbulence and mixing between the phases is well known. In recent years this mechanism has been utilised for gas-liquid or liquid-liquid mixing in straight tubes [1-4]. The momentum of the jet is utilised for dispersion of one phase into the other, for intense mixing between the phases and for continuous renewal of the interface. The effect of this mechanism on two phase mass and momentum transfer have been well emphasized and results are highly encouraging. However, very little work has been reported on heat transfer in such types of systems. It is expected that this mechanism may lead to the augmentation of heat transfer. Moreover, if such systems are to be designed for gas-liquid interfaces where energy transfer is also taking place, a knowledge of the two phase heat transfer coefficient is essential.

The present study deals with heat transfer in a two-phase water-air system in a horizontal circular tube with gas dispersion by shearing action of liquid jet.

### POSITION OF THE PROBLEM

The heat transfer coefficients for the two phase flow system have been calculated from an equation derived by applying a macroscopic heat balance over a control volume of the test section and assuming 100% saturation of air as it flows through the test section. The application of energy balance to the control volume gives,

$$q_1 + q_2 = q_3, \quad (1)$$

\*Present address: M/s APV Engineering Company, 2,  
Jessore Road, Calcutta-700028, India.

where

$$\begin{aligned} q_1 &= \text{rate of heat transfer into the control volume} \\ &\quad \text{by fluid flow} \\ &= Mc_p T|_x + M'c'_p T|_x, \end{aligned} \quad (2)$$

$$q_2 = \text{rate of heat transfer into the control volume by convection}$$

$$\text{and} \quad = h_{TP} \pi D \Delta x (T_w - T), \quad (3)$$

$$\begin{aligned} q_3 &= \text{rate of heat transfer out of the control} \\ &\quad \text{volume by fluid flow} \\ &= Mc_p T|_{x+\Delta x} + M'c'_p T|_{x+\Delta x}. \end{aligned} \quad (4)$$

Substitution of equations (2)–(4) in equation (1) and its rearrangement and evaluation within the limit  $x \rightarrow 0$  gives

$$Mc_p \frac{dT}{T_w - T} + M'c'_p \frac{dT}{T_w - T} = h_{TP} \pi D dx. \quad (5)$$

Integrating the equation (5) within the limits shown, we get

$$Mc_p \int_{T_i}^{T_s} \frac{dT}{T_w - T} + M'c'_p \int_{T_i}^{T_s} \frac{dT}{T_w - T} = h_{TP} \pi D \int_0^x dx. \quad (6)$$

It may be mentioned here that the upper limit of integration for the temperature for both gas and liquid has been taken as  $T_s$ . This is because in such systems it has been reported [5] that intense mixing takes place between liquid and gas. Thus gas gets dispersed uniformly and bubble flow is maintained in the system. Equation (6), on further simplification and rearrangement, leads to

$$h_{TP} = \frac{kRe_T Pr}{4x} \ln \frac{T_w - T_i}{T_w - T_s} + \frac{M'c'_p}{Dx} \ln \frac{T_w - T_i}{T_w - T_s}. \quad (7)$$

The fluid properties needed for the evaluation of  $h_{TP}$  at a particular section from equation (7) have been calculated at the average of the inlet temperature and the temperature at that section. The specific heat of air has been evaluated from the relation [6]

$$c'_p = 0.24 + 0.45H. \quad (8)$$

The variables that will affect the two phase heat transfer coefficient are classified in the following different groups:

#### Geometry of the system

The diameter of the nozzle,  $d$ , the diameter of the pipe,  $D$ , and the axial distance from the point of commencement of gas–liquid mixing,  $x$ , fall in this group. The axial distance is important because mixing is not uniform along the length of the test section.

#### Properties of the liquid

The specific heat,  $c_p$ , the conductivity,  $k$ , the density,  $\rho$ , and the viscosity,  $\mu$ , are the physical variables that will affect heat transfer.

#### Properties of the gas

The specific heat,  $c'_p$ , and the density,  $\rho'$ , are the physical variables which have been considered.

These physical properties have been changed by changing the working temperature of the system and have been taken into account.

#### Dynamic conditions

They may be defined as the velocity of the liquid through the nozzle,  $u$ , the velocity of air,  $u'$  and the pressure drop in the two phase flow system,  $\Delta P$ .

Since, in two phase heat transfer studies, it is customary to express the heat transfer coefficient as the augmentation ratio, i.e. ratio of  $h_{TP}$  to  $h_F$ , it may be written that

$$\frac{h_{TP}}{h_F} = f(d, D, x, c_p, k, \rho, \mu, c'_p, \rho', u, u', \Delta P, g_c). \quad (9)$$

Dimensional analysis would then lead to

$$\frac{h_{TP}}{h_F} = f(Re_N, Pr, Eu', A_R, x/D, de/d, \rho'/\rho, u'/u). \quad (10)$$

Since the ratio of diameters  $de/d$  is directly related to  $A_R$ , equation (10) reduces to

$$\frac{h_{TP}}{h_F} = f(Re_N, Pr, Eu', A_R, u'/u, x/D, \rho'/\rho). \quad (11)$$

#### EQUIPMENT AND GENERAL PROCEDURE

Figure 1 is a schematic diagram of the equipment, the dimensions of which are summarised in Table 1.

The equipment consists of a nozzle chamber, J, a horizontal test section, SS, and other accessories like centrifugal pump, P, air compressor, C, gas cylinders A and B, pressure gauges G and G', control valves V<sub>1</sub>–V<sub>13</sub>, the separator tank SP, the heating arrangements and thermocouples  $t_1$ – $t_5$ , etc. The forcing nozzle, N, is of straight hole type is precision bored to obtain a smooth passage and to avoid any undue shock and losses. It was fitted in the nozzle chamber at an optimum position [7] of 1.27 cm from the commencement of the test section. To find the effect of  $x/D$ , the test section was divided in five sections, 1–5, the  $x/D$  values of which are given in Table 2. Thermocouple pockets were provided to measure the average temperature at each section. For maintaining constant wall temperature each section was heated by a separate electric circuit to enable heat input in any section according to requirement. To avoid conduction heat losses from the test section the separator and jet chamber were separated from the test section by small thin Teflon tubes. The measurement of both wall and fluid temperatures at various different points have been carried out with copper–constantan thermocouples.

At the start of the experiment the water jet was formed and was found to move a long distance in the test section before disintegration. In order to utilise the

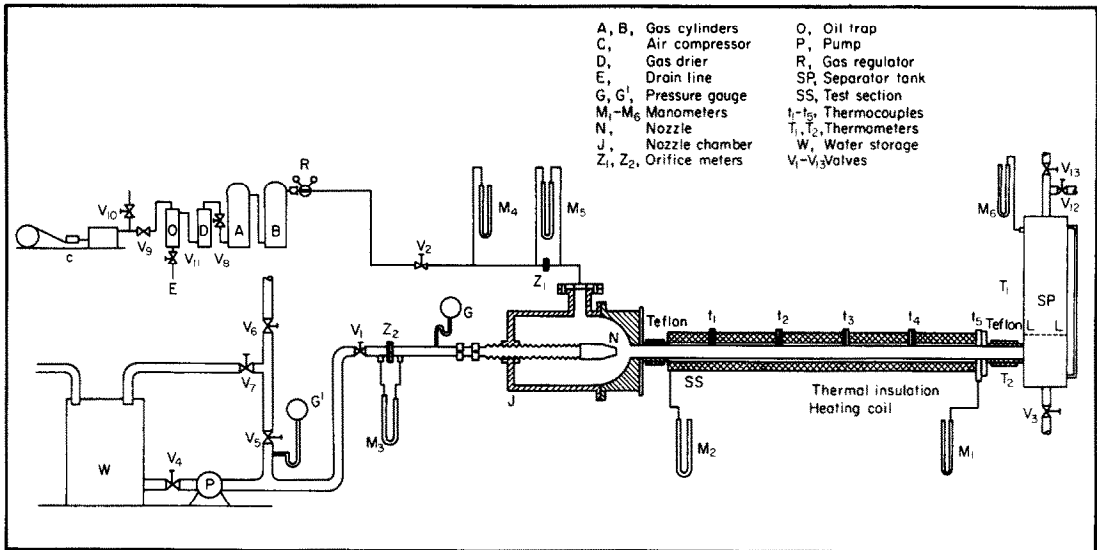


FIG. 1. Experimental set-up.

Table 1. Dimensions of nozzles

Serial number	Type of nozzles	Nozzle number	Nozzle diameter $d$ (cm)	Tube diameter $D$ (cm)	Area ratio $A_R = (D/d)^2$
1	Straight hole type	1	0.4366	2.54	33.85
2		2	0.3788		44.96
3		3	0.3175		64.00

Table 2. Distance of measuring point from point of entry

Section number	Distance $x$ (cm)	Tube diameter $D$ (cm)	$x/D$
1	45.7	2.54	18.0
2	91.5		36.0
3	137.2		54.0
4	182.9		72.0
5	228.6		90.0

jet momentum for efficient heat transfer, it was arrested at the beginning of the test section. This was achieved by filling up the separator, SP, and the test section, SS, with water by controlling the valve,  $V_3$ . At this condition there was single phase flow through the test section and the level of water in the separator was at L-L. Any attempt to change this level either caused flooding in the jet chamber or disintegration of jet [3]. Next, air was allowed to enter through the secondary inlet needle valve,  $V_2$ . This caused some disturbance in the level of the separator and it was readjusted to the same level L-L which ensured the arresting of the jet at the beginning of the test section. When the steady state was reached, the heating commenced. The variacs were adjusted to maintain a constant wall temperature all through the test section. The data on gas flow rate, water flow rate, two phase pressure drop in the test section and the temperature at various sections have been obtained at steady condition. It may be interest-

ing to mention here that the temperatures  $T_1$  and  $T_2$  of the air and the liquid in the separator were almost the same, within  $\pm 0.2^\circ\text{C}$ . Experiments have been conducted with three different nozzles, at water flow rate ranging from 300 to 1000  $\text{kg h}^{-1}$  and air flow rate from 1 to 5  $\text{kg h}^{-1}$ . The maximum wall temperature was kept at  $45^\circ\text{C}$  when most of the heat transferred goes into sensible heating and not into evaporation.

#### EXPERIMENTAL RESULTS AND DISCUSSIONS

A typical plot showing the axial temperature distribution is given in Fig. 2. It may be seen that the temperature rises rapidly at the beginning of the test section but the rate of rise of temperature decreases with increase in the distance of the point of measurement. This is attributed to the fact that intense mixing between the gas and liquid takes place at the beginning of the test section which decreases with the increase in  $x/D$ .

The  $h_{TP}$  values at different sections have been calculated from equation (7) and a typical plot showing the effect of air flow rate at section 3 at a constant liquid flow rate is given in Fig. 3. It is found that the two phase heat transfer coefficient increases with increase of air flow rate and then decreases. The initial increase in  $h_{TP}$  values may be attributed to uniform gas dispersion in the form of bubble flow with increase in air flow rate. The subsequent fall in  $h_{TP}$  values with further increase in air flow rate may be due to coalescence forming bigger bubbles. Similar obser-

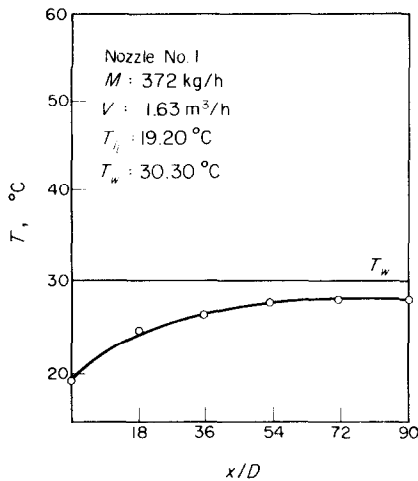


FIG. 2. Axial temperature distribution in the test section.

vation has also been reported by Johnson and Abou-Sabe [8].

For finding the augmentation ratio, the  $h_F$  values at different sections have been calculated by the Dittus–Boelter equation for single phase flow:

$$\frac{h_F D}{k} = 0.023 (Re_T)^{0.8} (Pr)^{0.4}. \tag{12}$$

Figure 4 shows a typical plot of the effect of air flow rate on the augmentation ratio at a constant liquid flow rate. As expected augmentation ratio showed similar behaviour as discussed in the previous paragraph. It may be seen, however, that at a constant air flow rate, the augmentation ratio increases with liquid flow rate and then again decreases. This may be explained qualitatively by the consideration that gas dispersion by liquid jet momentum reaches a maximum value which is not affected by further increase in water

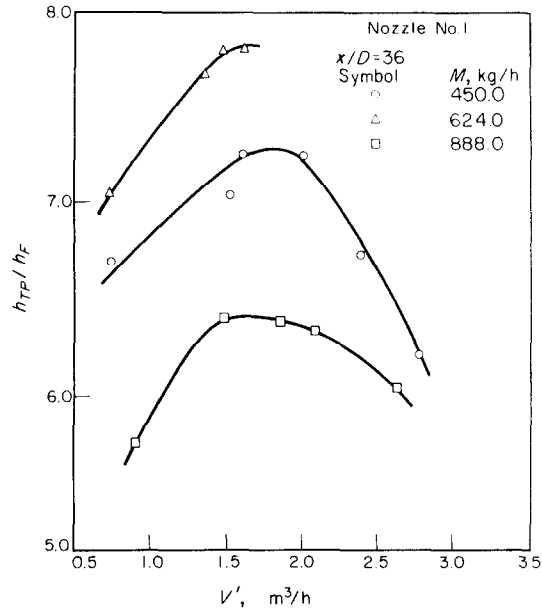


FIG. 4. Effect of volumetric flow rate of air on  $h_{TP}/h_F$ .

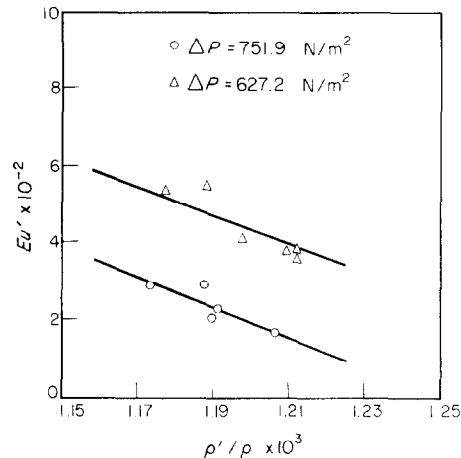


FIG. 5. Relation between  $p'/\rho$  and  $Eu'$  at constant  $\Delta P$ .

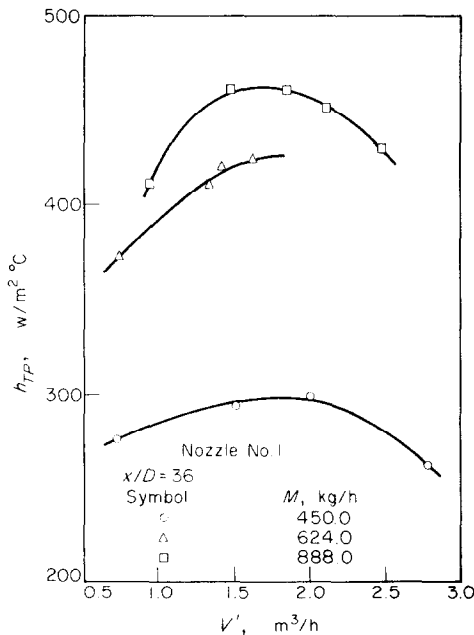


FIG. 3. Effect of volumetric flow rate of air on  $h_{TP}$ .

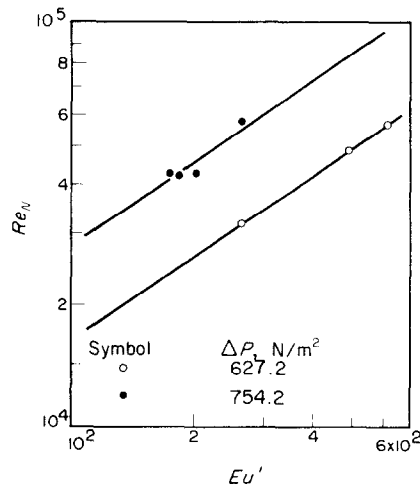


FIG. 6. Relation between  $Eu'$  and  $Re_N$  at constant  $\Delta P$ .

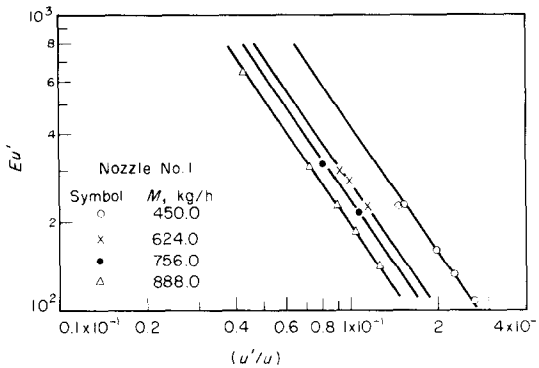


FIG. 7. Relation between  $Eu'$  and  $u'/u$  at constant liquid flow rate.

flow rate. At this stage though, increase in liquid flow rate with constant air rate causes increase in both  $h_{TP}$  and  $h_F$  values but the rate of increase of  $h_{TP}$  is much less compared to  $h_F$  values. Hence the augmentation ratio decreases. Similar observation has been reported by Johnson and Abou-Sabe. Direct comparison is difficult because the Johnson and Abou-Sabe study used very high flow rates of liquid and gas. However, at a comparable flow rate of  $450 \text{ kg h}^{-1}$  and air flow rate of  $2.5 \text{ m}^3 \text{ h}^{-1}$  the augmentation ratio obtained in this study was 6.5 which is much higher than the value of 1.9 obtained by Johnson and Abou-Sabe.

In order to correlate the experimental data on the lines of equation (7), plots were made for eliminating any possible interaction between the variables. Figures 5–7 show such plots where it is found that  $Eu'$  is directly proportional to  $Re_N$  and inversely proportional to  $u'/u$  and  $\rho/\rho'$ .

Hence, taking these relations into consideration equation (11) reduces to

$$\frac{h_{TP}}{h_F} = f(Eu', Pr, A_R, x/D), \quad (13)$$

which comes out as the complete representation of the augmentation ratio in terms of the independent variables for heat transfer in jet mixing with secondary flow of air.

#### EFFECT OF THE EULER NUMBER

The effect of the Euler number on the augmentation ratio has been determined for a constant Prandtl number, constant area ratio and  $x/D$  by varying air velocity.

Figure 8 presents typical plots of the experimental results. It shows clearly that, in a logarithmic plot, data can be conveniently represented by straight lines. The augmentation ratio increased slowly with the Euler number of the secondary fluid.

#### EFFECT OF PRANDTL NUMBER

The effect of the Prandtl number on the augmentation ratio has been determined by using the same nozzle and taking readings at one section keeping the air velocity the same and by varying the temperature.

Figure 9 presents some plots. It shows clearly that the augmentation ratio increases rapidly with the Prandtl number of the liquid and can be represented by straight lines in logarithmic plots.

#### EFFECT OF THE AREA RATIO

Three different nozzles were used in this investigation. The Euler number and the Prandtl number were kept constant and observations were taken at different  $x/D$ . Typical plots are shown in Fig. 10.

Although the results are not so clear, it can be seen that the augmentation ratio decreases with increasing area ratio. This is expected since better dispersion is obtained with bigger nozzles.

#### EFFECTS OF THE AXIAL DISTANCE OF THE TEST SECTION

Measurements at five different  $x/D$  values were taken for this purpose. The Euler number and the Prandtl number were kept almost the same and observations were taken with three different nozzles.

Typical plots are shown in Fig. 11. It can be seen that the augmentation ratio decreases with increasing distance of the test section. The logarithmic plot clearly shows a straight line relationship. This is also expected since the  $h_{TP}$  value increases with distance up to a certain maxima during which  $h_F$  also increases as the temperature of the system goes up. After this  $h_{TP}$  falls but  $h_F$  remains practically constant.

#### ANALYSIS OF DATA

The preceding graphical representations constitute only a first approach to the problem of heat transfer in horizontal pipe flow with jet mixing. Indeed it must be recalled that the parameters have been kept constant only approximately. However, this first study clearly shows that a power law type equation would conveniently represent the correlations between the dimensionless groups involved, i.e.

$$\frac{h_{TP}}{h_F} = A Eu^{b_1} Pr^{b_2} A_R^{b_3} (x/D)^{b_4}. \quad (14)$$

The numerical treatment of the 345 experimental data at five different  $x/D$  has been done with the help of digital computer EC 1030 using the least square technique. This treatment leads to

$$\frac{h_{TP}}{h_F} = 14.496 Eu^{0.045} Pr^{1.638} A_R^{-0.682} (x/D)^{-0.432}. \quad (15)$$

With a  $t$  value of 1.96 for 340 d.f. at 0.05 level, the 95% confidence range on the regression coefficients are:

$$b_1: 0.045 \pm 0.0006,$$

$$b_2: 1.638 \pm 0.0616,$$

$$b_3: -0.682 \pm 0.0032,$$

$$b_4: -0.432 \pm 0.0006.$$

For the verification of the null hypothesis, i.e. whether the correlation is significant or not, the  $F$

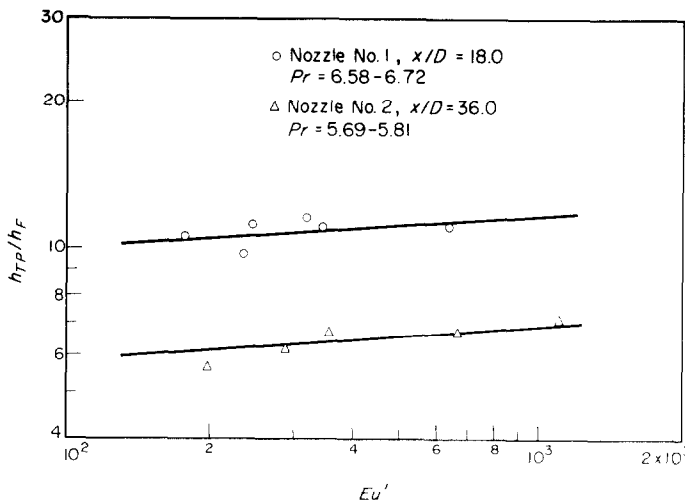


FIG. 8. Effect of  $Eu'$  on  $h_{TP}/h_F$ .

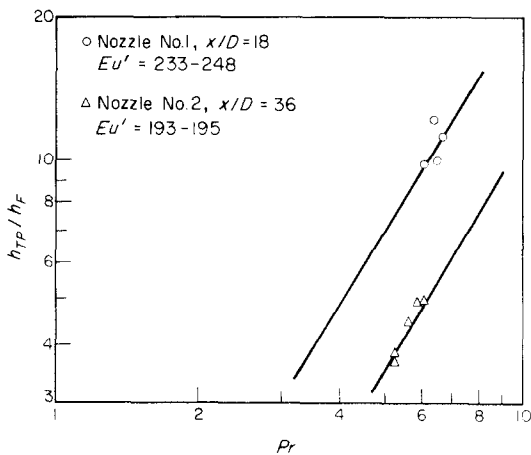


FIG. 9. Effect of  $Pr$  on  $h_{TP}/h_F$ .

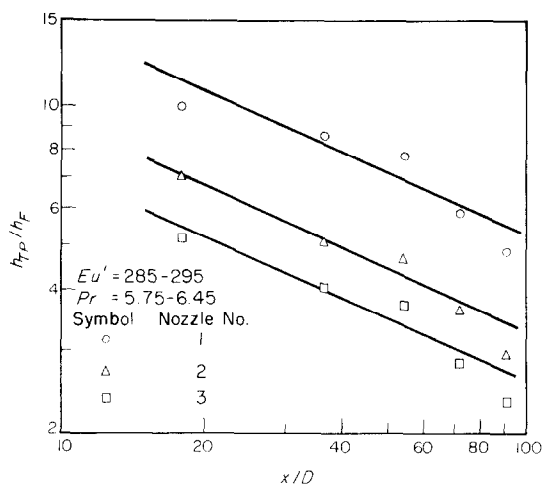


FIG. 11. Effect of  $x/D$  on  $h_{TP}/h_F$ .

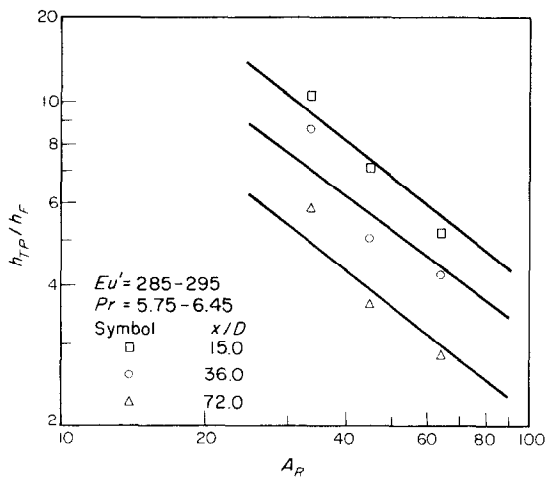


FIG. 10. Effect of  $A_R$  on  $h_{TP}/h_F$ .

value has been calculated. The value obtained is equal to 294.542, which is much bigger than the specified value of  $F_{0.01} = 3.36$ . Hence the null hypothesis may be rejected and it may be concluded that the correlation is highly significant at the 99% confidence

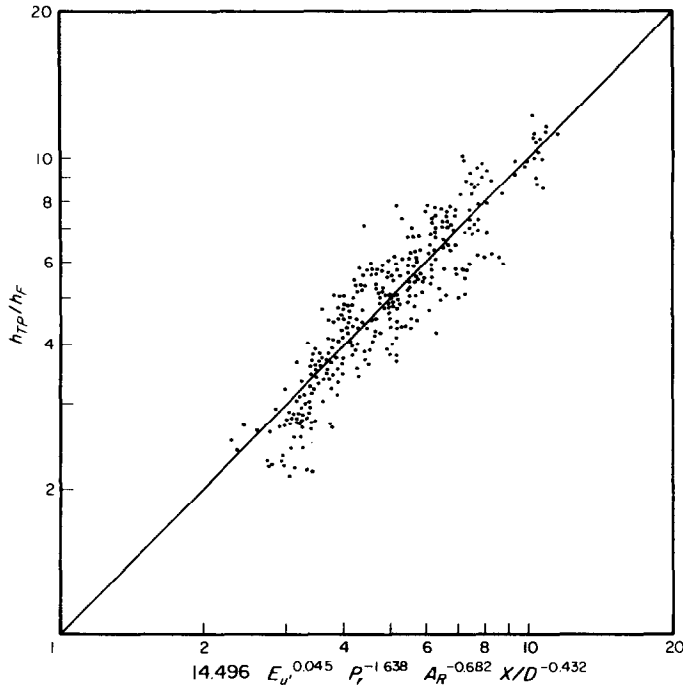
level. The correlation coefficient has also been calculated and is of the order of 0.881.

A plot of the experimental and calculated values of  $h_{TP}/h_F$  is shown in Fig. 12 where the range of variation of different parameters are as follows:

$$\begin{aligned} 100 < Eu &< 1600, \\ 4 < Pr &< 7, \\ 33 < A_R &< 64, \\ 18 < x/D &< 90. \end{aligned}$$

CONCLUSION

Liquid jet momentum had been utilised for gas dispersion and mixing. It has been found that this technique can also be used in augmenting the heat transfer coefficient in two phase horizontal flow. In the present range of investigations augmentation ratios as high as 12 have been obtained. A correlation predicting the augmentation ratio was proposed which, under the present range of parameter variations, may be used with 99% confidence level.

FIG. 12. Experimental vs calculated values of  $h_{TP}/h_F$ .

## REFERENCES

1. M. L. Jackson, Aeration in Bernoulli types of devices, *A.I.Ch.E.Jl* **10**(6), 836–842 (1964).
2. D. K. Acharjee, A. K. Mitra and A. N. Roy, Cocurrent flow liquid–liquid binary mass transfer in ejectors, *Can. J. Chem. Engng* **56**(1), 37–42 (1978).
3. M. N. Biswas, A. K. Mitra and A. N. Roy, Studies on gas dispersion in a horizontal liquid-jet ejector, *2nd Symposium on Jet Pumps, Ejectors and Gas-Lift Techniques*, BHRA, March 24th–26th (1975).
4. A. K. Mitra and H. Brauer, Optimisation of a two-phase cocurrent flow nozzle for mass transfer, *Verfahrenstechnik* **7**(4), 92–97 (1973).
5. P. A. Bhat, A. K. Mitra and A. N. Roy, Momentum transfer in a horizontal liquid-jet ejector, *Can. J. Chem. Engng* **50**(6), 313–317 (1972).
6. R. E. Treybal, *Mass Transfer Operations*, p. 188. McGraw-Hill–Kogakusha Ltd., Tokyo (1968).
7. K. P. Singh, N. K. Purohit and A. K. Mitra, Performance characteristics of an horizontal ejector, water–water system, *Ind. Chem. Engr.* **16**(3), 23–28 (1974).
8. H. A. Johnson and A. H. Abou-Sabe, Heat transfer and pressure drop for turbulent flow of air–water mixtures in a horizontal pipe, *Trans. Am. Soc. Mech. Engrs* **74**(8), 977–987 (1952).

### TRANSFERT THERMIQUE DANS UN TUBE HORIZONTAL AVEC MELANGE DIPHASIQUE PAR JET

**Résumé**—Le texte concerne les études expérimentales sur le coefficient de transfert pour l'écoulement diphasique à contre-courant dans un tube horizontal où la quantité de mouvement du jet liquide est utilisée pour la dispersion et le transfert thermique gaz–liquide. Des équations empiriques sont proposées pour prévoir l'augmentation du transfert thermique en fonction des paramètres physiques et dynamiques du système.

### ZWEIPHASENWÄRMEÜBERGANG IN EINEM HORIZONTALEN ROHR MIT DÜSENMISCHUNG

**Zusammenfassung**—Die Abhandlung befaßt sich mit experimentellen Untersuchungen über den Wärmeübergangskoeffizienten einer Zweiphasenströmung in einem horizontalen Rohr, in dem der Impuls eines Flüssigkeitsstrahls zur Mischung von Gas und Flüssigkeit und zur Intensivierung des Wärmeübergangs dient. Empirische Gleichungen wurden aufgestellt, welche die Zunahme des Wärmeübergangs als Funktion von verschiedenen physikalischen und dynamischen Einflußgrößen des Systems wiedergeben.

### ДВУХФАЗНЫЙ ТЕПЛОПЕРЕНОС В ГОРИЗОНТАЛЬНОЙ ТРУБЕ ПРИ СТРУЙНОМ ПЕРЕМЕШИВАНИИ

**Аннотация** — Проведено экспериментальное определение коэффициента теплопереноса при спутном течении двухфазной жидкости, диспергированной газом, в горизонтальной трубе. Получены эмпирические уравнения для расчета зависимости интенсификации теплопереноса от различных физических и динамических переменных системы.